NASA Technical Paper 2301

April 1984

Homogeneous Reactions of Hydrocarbons, Silane, and Chlorosilanes in Radiofrequency Plasmas at Low Pressures

Reuven Avni,
Uzi Carmi,
Aron Inspektor,
and Ionel Rosenthal

NASA

NASA
Technical
Paper
2301

1984

Homogeneous Reactions of Hydrocarbons, Silane, and Chlorosilanes in Radiofrequency Plasmas at Low Pressures

Reuven Avni
Lewis Research Center
Cleveland, Ohio

Uzi Carmi,
Aron Inspektor,
and Ionel Rosenthal
Nuclear Research Center Negev
Beer Sheva, Israel

NASA
National Aeronautics
and Space Administration

**Scientific and Technical
Information Branch**

Summary

The ion-molecule and radical-molecule mechanisms are responsible for the dissociation of hydrocarbon, silane, and chlorosilane monomers and the formation of polymerized species, respectively, in an rf plasma discharge. In a plasma containing a mixture of monomer and argon the rate-determining step for both dissociation and polymerization is governed by an ion-molecule type of interaction. Adding hydrogen or nitrogen to the monomer-argon mixture transforms the rate-determining step from an ion-molecule interaction to a radical-molecule interaction for both monomer dissociation and polymerization.

Introduction

Hydrocarbons and chlorosilanes (silane or organosilicones) are the monomers from which refractory compounds or composite ceramic materials such as carbon-carbons (refs. 1 and 2), silicon-carbides (refs. 3 and 4), and silicon nitrides (refs. 5 and 6) are produced. Chemical vapor deposition (CVD) (refs. 7 to 9) and plasma processing (or plasma-activated CVD) (refs. 10 and 11) are techniques used in forming these materials and in improving the ceramic products obtained by other techniques such as sintering, reaction bonding, and hot pressing. Since these ceramics are potential materials for the transportation industry (refs. 12 to 14) and in semiconductors (refs. 15 and 16), better control of the refractory compound fabrication process is essential. Understanding the homogeneous and heterogeneous reactions occurring in the plasma (or gas) state and in the plasma-substrate region is a necessity for better control.

In radiofrequency (rf) discharges hydrocarbons such as methane, acetylene, and propylene (refs. 17 and 18) polymerize and form solid pyrocarbon (refs. 19 to 21). In similar discharges silane (refs. 22 to 25) or chlorosilanes (refs. 26 to 30) form solid silicon. Adding ammonia to silane or chlorosilanes in an rf plasma results in the deposition of Si_3N_4 (refs. 31 and 32); organosilicones such as tetrametyl silane (ref. 33) in an argon rf plasma form solid SiC. Introducing rare gases (Ar or He) into an rf plasma enchances the dissociation of the monomer, its polymerization, and the deposition of both pyrocarbon (refs. 19 to 21 and 34 to 36) and silicon (refs. 23 to 29). In an rf discharge argon, playing the role of a charge carrier, enhances the ionization of hydrocarbon species by charge transfer reactions and by Penning ionization (refs. 19 to 21). The presence of argon in the discharge enhances, as well, the deposition rate on grounded or negatively biased substrates (refs. 17 to 21).

The aim in the present work is to shed more light on the nature of the mechanism and kinetics in the homogeneous reactions of hydrocarbons and chlorosilanes in rf plasmas—in other words, to find the rate-determining steps in dissociating the monomer and forming the polymerized species. Two different plasmas, one containing the monomer mixed with argon and the other containing hydrogen (or ammonia) as well, were diagnosed and compared by the following characteristics:

(1) Mean electron energy T_e and plasma density n_i

(2) Overall reaction rate k_o and local reaction rate k_L for monomer dissociation and formation of polymerized species, respectively, in different locations in the plasma

(3) Relative concentration of free radicals in different locations in the plasma

(4) Deposition rate as measured on floating, grounded, and biased (-100 V) solid substrates

These diagnostics were performed by varying plasma parameters such as total gas pressure, relative concentration of the monomer in the gas mixtures (i.e., its partial pressure), and net power input to the plasma at different locations in the plasma and at constant flow velocity.

Two general mechanisms of homogeneous reactions are found in the literature:

(1) Positive ion-molecule reactions (refs. 34 to 41)

(2) Radical-molecule reactions (refs. 43 to 45).

Which of the two mechanisms is rate determining in the homogeneous or the heterogeneous reactions in a given plasma system has not yet been solved. Both mechanisms are considered in the present work.

To discern which of the two mechanisms is rate determining in a plasma system, a general criterion is needed. Free radicals, positive ions, and negative ions are continuously formed in the plasma as a result of the interaction of the gas monomer molecules with the plasma's energetic electrons. The concentrations per unit volume of plasma (cm^{-3}) of free radicals n_R, positive ions n_i, and negative ions n_N and their spatial gradients

are variables entering into the kinetics of reactions with monomer molecules. Another variable controlling the kinetics is the reactivity of the radicals and the charged ions (i.e., the cross sections σ_R, σ_i, and σ_N of such reactions). The probability P is defined as the product of n and σ in a given location z along the plasma system. Thus if $n_R\sigma_R > n_i\sigma_i$, then $P_R > P_i$ and the probability of radical-molecule interaction is higher than the probability of ion-molecule interaction at z, and vice versa for $n_i\sigma_i > n_R\sigma_R$ at z.

Experimental Procedure

The rf plasma was induced by an rf coil wound around a 13-cm-diameter Pyrex reactor energized by a 13.56-MHz generator as described in references 21 and 40. The reactor was kept at constant conditions by adjusting the composition and flow of the gas mixture while maintaining the desired pressure between 1.0 and 10.0 torr. Starting materials for the hydrocarbon plasma were C_3H_6 (CP, Matheson) and argon (UHP, Matheson). For the silicon or silicon nitride plasma, $SiCl_4$ vapor was introduced from its liquid (UP, Alfa Venturon) by using argon as the carrier gas. Additional argon, hydrogen (UHP, Matheson), and ammonia (arhydrous, 99.99 percent, Matheson) were mixed with the $SiCl_4$-saturated argon as necessary. Three positions were established and considered as shown in figure 1(a): position H—upstream, at the beginning of the plasma, where the fresh reactants approached the rf coil; position G—at the center of the rf coil, where maximum energy density was delivered to the plasma; and position F—downstream, where unreacted gases left the plasma. Positions H, G, and F were 5.0 cm apart, which in terms of time, at 10.0 torr for example, means that they were 45 ms apart at the given flow rate and pumping speed (refs. 40 and 45). This is referred to as the overall reaction time τ_o.

Four methods were used to characterize the plasma:

(1) Double floating probes system (DFPS): This is a simple method whereby the values of electron energy T_e and ion density n_i can be evaluated. Essentially the method consists of inserting two tungsten probes into the plasma and measuring the volt-ampere characteristics. The setup and measuring procedures are quite simple, but the physical and mathematical evaluations of T_e and n_i are somewhat elaborate and are described elsewhere (ref. 21).

(2) Quadrupole mass spectrometry (QMS): In this method species from the plasma are extracted to the analyzing mass spectrometer by differential pumping through two small (200 μm) orifices. The fully detailed experimental data were presented previously (ref. 45). From the interpretation of the mass spectrometric data, kinetic information in the plasma can be obtained. By

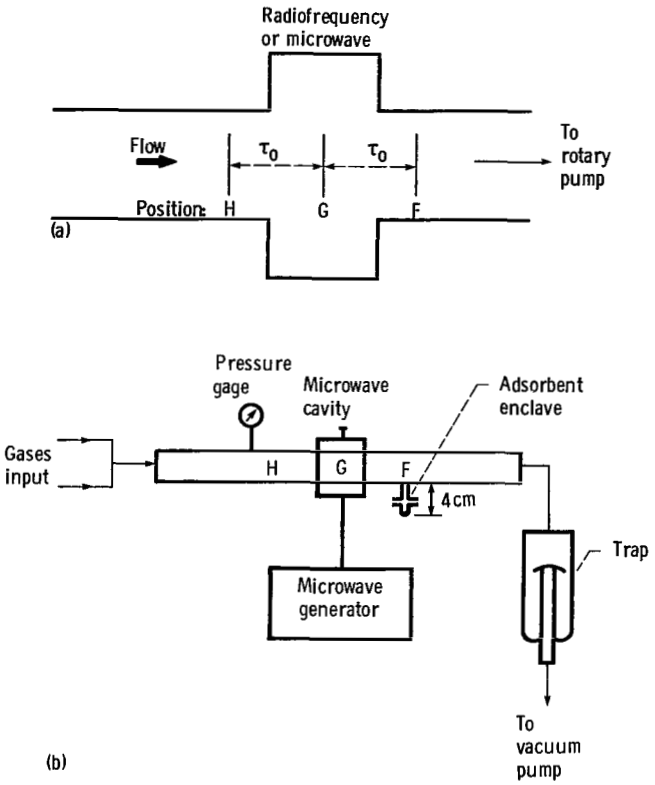

(a) Locations H, G, and F in plasma with regard to rf coil and gas flow. (Overall reaction time τ_o is the time spent by the monomer between H, G, and F.

(b) Experimental setup for adsorbing free radicals from plasma. (Adsorbing enclave is shown in position F.)

Figure 1. – Experimental apparatus.

considering different plasma parameters, two kinds of kinetic constants were evaluated. The overall reaction rate constant k_o was evaluated from the plot of the m/e normalized concentration $I/\Sigma I$ of each monomer mass peak versus its position in the plasma. The local reaction rate constant k_L (ref. 46) was evaluated from a plot of each mass species $I/\Sigma I$ versus pressure.

In the $SiCl_4$ plasma, hydrogen or ammonia was introduced by mixing it with the additional argon at a known concentration. In the hydrocarbon plasma on the other hand, hydrogen was evolved from the fragmentation of the hydrocarbons, and its concentration in the plasma was measured by its mass spectrometric peak height. No additional hydrogen was added. The hydrogen concentration in the hydrocarbon plasma was varied by varying the amount of C_3H_6 in the argon flow (4 percent H_2 from 16 vol% C_3H_6 and 12 percent H_2 from 66 vol% C_3H_6 (refs. 19 and 40).

(3) Electron parametric resonance (EPR): The radical concentration in the plasma was indirectly determined by using an EPR spectrometer. Figure 1(b) shows a schematic setup for EPR sampling in position F. Radicals from the plasma were adsorbed and stabilized on alu-

mina. The alumina was pretreated in the reactor enclave by slowly heating and degasing it before connecting it to the plasma system. Sampling at the various plasma positions (H, G, and F) was achieved by moving the rf coil along the reactor. The plasma was activated for a fixed time and radicals were adsorbed by the alumina. Before each set of experiments a blank sampling was taken for comparison. After each sampling process the alumina was transferred to an EPR tube and the EPR spectrum was recorded. Since the radicals were adsorbed on the solid, the resolution of the EPR spectrum was poor and different radicals could not be identified. However, the peak intensity served as an indicator for the relative radical concentration in the plasma.

(4) Deposition rate: The deposition rate of silicon or pyrocarbon was evaluated by inserting a solid substrate into the plasma for a fixed time. Pyrocarbon was deposited on commercial ATJ graphite placed at position F. Silicon and Si_3N_4 were deposited on a similar graphite substrate and on stainless martensitic steel (AISI-410), both at position H. The significance and reasoning for placing the two substrates at the various locations in the plasma are discussed by Manory et al. (ref. 45). Both substrates were mounted on a metal rod extending out of the reactor so that the substrates could be left floating, grounded by earth connection, or connected to an external dc power source for biasing.

Deposition rates of pyrocarbon, silicon, and Si_3N_4 were evaluated by thickness measurements as dh/dt (μm h^{-1}), where h is thickness and t is time. Corrections were made for the inequality of deposition rate on the two sides of the substrates. The coated substrates were cut and polished and the thicknesses were measured on the section by optical microscope (and by SEM for Si_3N_4 coatings).

Results and Discussion

Electron Energy and Plasma Density

In position G, at the center of the rf coil (maximum energy density delivered to the plasma), at 100-W net power input, adding hydrogen or ammonia to the plasma inhibited the values of both mean electron energy T_e and positive ion density n_i as shown by the ratios (smaller than 1.0) in table I. For the $SiCl_4$-argon plasma when hydrogen or ammonia was added, the inhibition effects on T_e and n_i were stronger than the effect of hydrogen on the C_3H_6-argon plasma. As shown in table I, the inhibition effect of hydrogen or ammonia increased with increasing pressure in the plasma (i.e., the inhibition was an inverse function of the mean free path of the interacting particles in the plasma).

The lower values of n_i in the presence of 20 vol% hydrogen or 15 vol% ammonia show an inhibition in the ionization process for the following reasons:

(1) The amount of energetic electrons (above 12 eV) needed for the ionization of $SiCl_4$ was reduced as shown by the lower T_e values in table I.

TABLE I. - ELECTRON ENERGY AND ION DENSITY RATIOS IN RADIOFREQUENCY OR MICROWAVE PLASMAS OF Ar, Ar + H_2, Ar + NH_3 AND Ar + N_2 GAS MIXTURES

[Input power, 100 W; position G.]

Pressure, torr	$\frac{C_3H_6(SiH_4) + H_2 + Ar}{C_3H_6(SiH_4) + Ar}$ [a]	$\frac{SiCl_4 + H_2(NH_3) + Ar}{SiCl_4 + Ar}$ [b]	$\frac{SiH_4 + N_2 + Ar}{SiH_4 + Ar}$ [c]
	Electron energy ratio, T_e		
2	0.83	0.91	1.00
4	.71	.65	.90
6	.66	.55	.90
	Ion density ratio, N_1		
2	0.77	0.43	0.95
4	.66	.30	.92
6	.53	.22	.96

[a] $\frac{(66\ vol\%\ C_3H_6 + 12\ vol\%\ H_2)/Ar}{(16\ vol\%\ C_3H_6 + 4\ vol\%\ H_2)/Ar}$

$\frac{(5\ vol\%\ SiH_4 + 10\ vol\%\ H_2)/Ar}{5\ vol\%\ SiH_4/Ar}$

[b] $\frac{[3.5\ vol\%\ SiCl_4 + 20\ vol\%\ H_2(15\ vol\%\ NH_3)]/Ar}{3.5\ vol\%\ SiCl_4/Ar}$

[c] $\frac{(5\ vol\%\ SiH_4 + 15\ vol\%\ N_2)/Ar}{5\ vol\%\ SiH_4/Ar}$

(2) The charge transfer reaction $Ar^+ + SiCl_4^+ \rightarrow SiCl_4^+ + Ar$ was partly replaced by excited Ar* particles and $H^\cdot$ radicals (refs. 47 and 48):

$$Ar^+ + H_2 \rightarrow (ArH)^+ + H^\cdot$$

$$ArH^+ + H_2 \rightarrow Ar + H_3^+$$

$$ArH^+ + e^- \rightarrow Ar^* + H^\cdot$$

$$H_3^+ + e \rightarrow H_2 + H^\cdot$$

Overall and Local Kinetics

The species obtained from the $SiCl_4$-argon-hydrogen (or ammonia) plasma and the $SiCl_4$-argon plasma are presented in figure 2 at various plasma positions. Similar plots were obtained for the C_3H_6 plasma and were published in reference 40. From figure 2 or similar plots (for $SiCl_4 + Ar + NH_3$ and $C_3H_6 + Ar$), the overall reaction rate k_o for the dissociation of the monomer ($I_{monomer}/\Sigma I$) and the formation of unidentified products was evaluated as follows (ref. 40): Because of the high excess of the monomer in the plasma the chemical reaction of the sort $M + S^{(+)(\cdot)} \rightarrow P$, where M is the reactant monomer, $S^{(+)(\cdot)}$ is some species in the plasma (ion or radical), and P is the products, can be considered a pseudo-first-order reaction in M and S. For the dissociation of M and the formation of P the overall kinetics apply. Since at all positions (H, G, and F) in the plasma steady-state conditions exist, the usual kinetic model applies:

$$\int_{\tau_o = 0 \text{ at } H}^{\tau_o \text{ at G}} d \ln (I/\Sigma I) = k_o \tau_o \qquad \text{for monomer}$$

The overall reaction rate k_o was evaluated from the slope of the plot of $I_{monomer}/\Sigma I$ versus position and the value of τ_o (as described in the section Experimental Procedure) for the distances H–G and G–F at given flow rates and pressure.

For the species S, whose residence time is considerably shorter, a different model for the rate constant was evaluated by Fields et al. (ref. 46). The final equation reads

$$k_L \tau_L P = \ln(I/\Sigma I)$$

where τ_L is the ion or radical residence time and P is the reactant partial pressure. Thus by plotting $\ln(I/\Sigma I)$ versus P, the slope $k_L \tau_L$ is evaluated (ref. 40). The ionic residence time can be evaluated by using its mobility and the Langevin relationship (refs. 49 and 50). The radical residence time was evaluated from its velocity and collision frequency.

The overall reaction rate constants k_o for the dissociation of C_3H_6 and $SiCl_4$ between positions H and G, for the rf plasma, are given in table II at 100 W and 1.0 torr. Because the concentration of hydrogen in the 66 vol% C_3H_6-argon plasma (refs. 19 and 40) was higher than that in the 16 vol% C_3H_6-argon plasma, monomer dissociation and the formation of products were inhibited by a factor of about 3. In other words, the direction of the homogeneous reaction was reversed:

$$C_3H_6 \underset{\text{high } (H_2)}{\overset{\text{low } (H_2)}{\rightleftharpoons}} \text{Products}$$

This behavior is shown as well in figure 3, where the overall reaction rate constant k_o of C_3H_6 increased when the concentration of C_3H_6 in the gas mixture ($C_3H_6 + Ar$) was decreased. When 100 vol% C_3H_6 was present in the plasma, its dissociation was due mainly to the interaction with the energetic plasma electrons, corresponding to $k_o = 50\ s^{-1}$ for a pressure of 1.0 torr. The hydrocarbon concentration in the gas stream was lowered by mixing

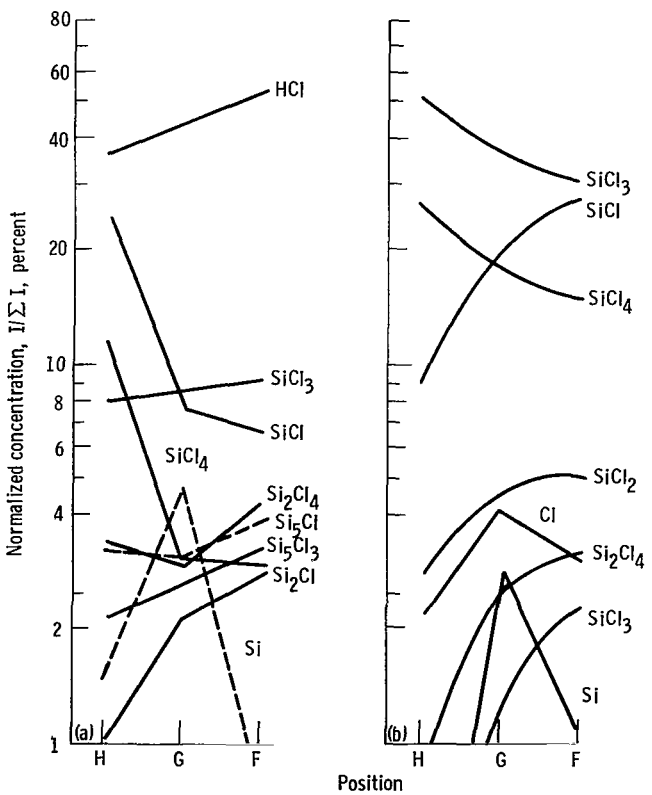

(a) 3.5 vol% $SiCl_4 + 20$ vol% $H_2 + Ar$.
(b) 3.5 vol% $SiCl_4 + Ar$.

Figure 2. – Normalized concentration of chlorosilane species for plasma sampled in three positions at 100 W and 4.0 torr.

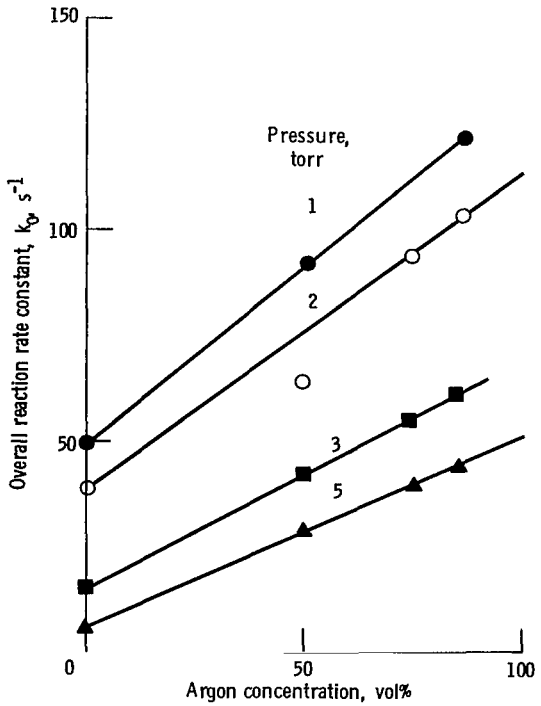

Figure 3. – Overall reaction rate constant as function of argon concentration in C_3H_6 plasma at 400 W and various pressures.

C_3H_6 with argon, and a charge transfer reaction from Ar^+ and Penning ionization occurred with the argon-excited metastable state (11.55 eV). Thus the dissociation rate of the monomer was enhanced.

As shown in table II, for the $SiCl_4$-argon plasma, adding hydrogen or ammonia enhanced the dissociation of $SiCl_4$ and the resulting products. The admixtures of 20 vol% hydrogen to 3.5 vol% $SiCl_4$ in argon enhanced k_o values about 40 times. For 15 vol% NH_3 the k_o values were enhanced about 25 times.

The values of k_L, the local reaction rate constant, for some of the products (polymers) in the plasma state, formed from the dissociation of the monomer, are shown in table III and figure 4. The rate of formation of the polymeric species, represented by C_4H_8, C_2H_2, and C_4H_4, etc., was hindered by hydrogen for a higher concentration of propylene in the C_3H_6-argon stream. Values of the local reaction rate ratio K_L were below 1.0 and were about the same order of magnitude as the values of the overall reaction rate ratio K_o (table II). This indicated that in the hydrocarbon plasma the dissociation and formation rates of the polymeric species are governed by the same mechanism (refs. 21 and 40). Comparing the results given in table III with those of figure 3, where the reaction rate constant increases with increasing argon concentration in the gas stream, might lead to the conclusion that an Ar^+ ion-molecule mechanism governs the kinetics of dissociation k_o as well as formation k_L of the polymerized molecules.

For the chlorosilane monomer the rate of formation of the polymerized silicon species was enhanced by adding hydrogen or ammonia in the gas stream, as shown in table III. In the $SiCl_4$ plasma the values of k_L were about one order of magnitude lower than the values of k_o from table II (i.e., $k_o > k_L$). Thus when hydrogen or ammonia is present in the $SiCl_4$-argon plasma, another mechanism besides the ion-molecule mechanism controls the values of both K_o and K_L for the chlorosilicones. The values of K_L in table III were derived by assuming an ion-molecule interaction for the τ_L calculation. To find out if a radical or positive ion mechanism was responsible for the dissociation of the monomer, the formation of polymerized species, and the deposition of silicon, Si_3N_4, and pyro-

TABLE II. - OVERALL REACTION RATE CONSTANTS (k_o) FOR THE DISSOCIATION OF C_3H_6, SiH_4, and $SiCl_4$

[Input power, 100 W; positions H → G: pressure, 1.0 torr: overall reaction time, τ_o, 2.2 m/s.]

Gas mixture, vol%	Plasma			$K_o = \frac{k_o(Ar + H_2)(NH_3)}{k_o(Ar)}$
	C_3H_6	SiH_4	$SiCl_4$	
	Overall reaction rate constant, k_o, s^{-1}			
16 C_3H_6 + Ar	228	---	---	0.26
66 C_3H_6 + Ar	60	---	---	
5.0 SiH_4 + Ar	---	330	---	.29
5.0 SiH_4 + 15 H_2 + Ar	---	95	---	
3.5 $SiCl_4$ + Ar	---	---	15	40.0
3.5 $SiCl_4$ + 20 H_2 + Ar	---	---	600	
3.5 $SiCl_4$ + 15 NH_3 + Ar	---	---	400	27.0

TABLE III. - LOCAL REACTION RATE CONSTANTS

[Input power, 100 W; pressure = 1 torr.]

(a) Position F

Plasma species	Plasma		Local reaction constant, $K_L = k_L/k'_L$
	66 vol% C_3H_6 + Ar	16 vol% C_3H_6 + Ar	
	Local reaction rate constant,[a] cm^3 $molecule^{-1}s^{-1}$		
	k_L	k'_L	(a)
$C_2H_2^+$	0.30×10^{-10}	1.9×10^{-10}	0.16
$C_2H_4^+$	1.10	1.5	.73
$C_4H_2^+$	.60	1.3	.46
$C_4H_4^+$	.05	.2	.25
$C_4H_8^+$	.08	.6	.13

(b) Position H

Plasma species	Plasma		Local reaction constant, $K_L = k_L/k'_L$
	3.5 vol% $SiCl_4$ + 20 vol% H_2 + Ar	3.5 vol% $SiCl_4$ + Ar	
	Local reaction rate constant,[b] cm^3 $molecule^{-1}s^{-1}$		
	k_L	k'_L	(b)
$Si_2Cl_2^+$	10.0×10^{-10}	4.0×10^{-10}	2.50
$Si_2CL_4^+$	23.0	3.7	6.20
$Si_3Cl_5^+$	8.8	5.0	1.76
$Si_5Cl_2^+$	5.0	3.0	1.66
Si_5Cl^+	4.0	2.8	1.43

[a]Same K_L values were obtained for silane species in 100 vol% SiH_4/5 vol% SiH_4 in argon.
[b]Same K_L values were obtained in 3.5 vol% $SiCl_4$ + 15 vol% NH_3 in argon and 3.5 vol% $SiCl_4$ in argon.

carbon, the probability criterion (see Introduction) should be applied.

The following experiments were performed:

(1) Electron paramagnetic resonance spectrometry for evaluating the free radical concentration n_R at a given location in the plasma

(2) Deposition rate on floating or grounded substrates The reason for performing these experiments is as follows: In general, the cross-section values for charge transfer reactions σ_i are in the range 10^{-15} to 10^{-16} cm^2 (refs. 50 and 51) and those for radical interactions σ_R are in the range 10^{-18} to 10^{-20} cm^2. Comparing only the closest extremes $\sigma_i = 10^{-16}$ cm^2 with $\sigma_R = 10^{-18}$ cm^2 (i.e., approx two orders of magnitude) allows the product to be compensated by $n_R = 10^2 n_i$ (refs. 42 and 43) at pressures above 1.0 torr, where $n_i = 10^{11}$ cm^{-3} (table I). For such conditions using the probability criterion means equal probability for both radical- and ion-molecule mechanisms.

Electron Paramagnetic Resonance (EPR)

Typical EPR spectra with and without hydrogen in the $SiCl_4$-argon plasma are shown in figure 5. The spectrum for ammonia is shown in reference 31. The behavior of the normalized EPR intensity of free radicals at the three plasma locations (H, G, and F) with increasing power is shown in figure 6. For the C_3H_6-argon plasma with 20 vol% hydrogen at the gas feed, increasing the induced power increased the normalized EPR intensity for positions H and G, but for position F EPR intensity peaked at 100 W. At 150 W the normalized amount of free radicals was about 15 times higher in position G than

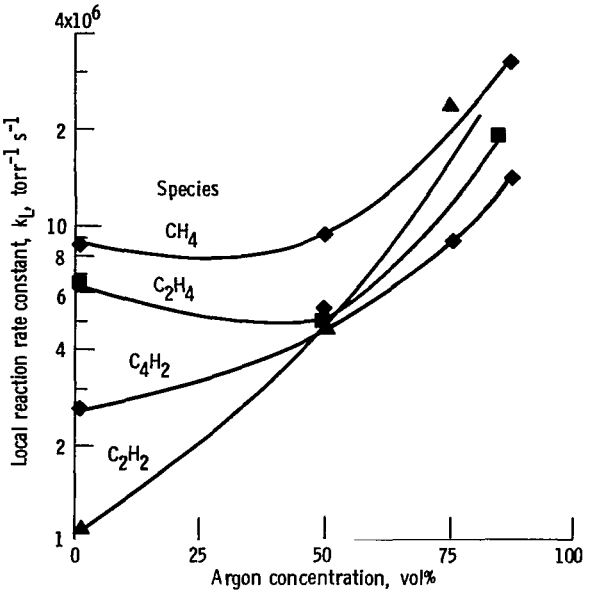

Figure 4. – Local reaction rate constant as function of argon concentration in C_3H_6 plasma at 100 W and 5.0 torr.

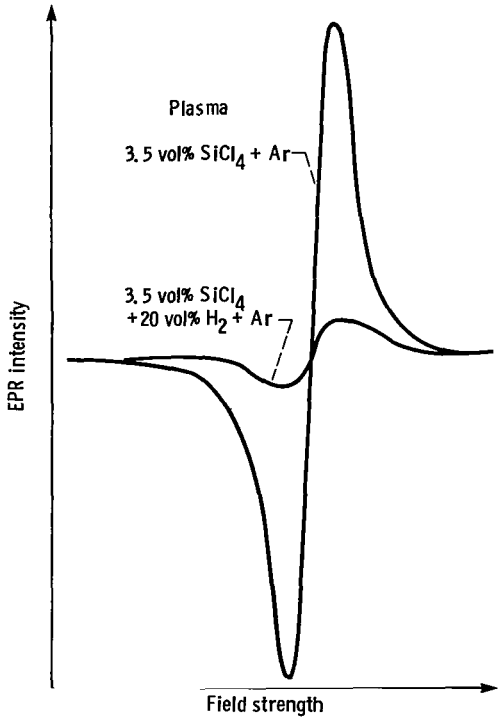

Figure 5. – EPR spectra of free radicals adsorbed on alumina.

in position H. Thus the formation of free radicals in the plasma with hydrogen started where the gases entered the plasma (position H), reached a maximum in position G due to the overall radical interaction, and declined toward position F. In the $SiCl_4$-argon plasma making similar additions of 20 vol% hydrogen (fig. 6) and

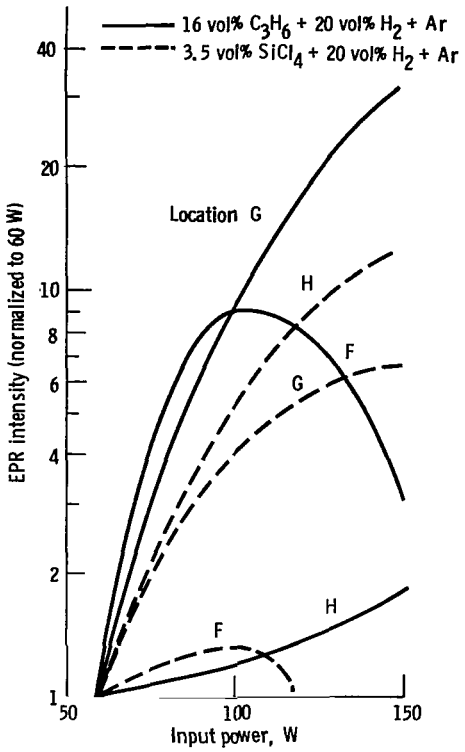

Figure 6. – Normalized EPR intensity of free radicals as function of input power.

varying the rf power produced a maximum normalized EPR intensity in position H, a lower intensity in position G (where the maximum energy density was introduced to the plasma), and a minimum intensity in position F. In other words, the normalized amount of free radicals was highest upstream, where the gases entered the plasma, and lowest downstream, where the gases, after reacting, left the plasma.

In a plasma of solely 20 vol% hydrogen and argon no free radicals were detected in the alumina. The H· radicals quickly recombine to hydrogen in alumina. Therefore the free radicals detected in plasma containing hydrogen and argon were only those due to the partial dissociation of $SiCl_4$ or C_3H_6. Moreover it should be remembered that adding 20 vol% hydrogen to a 16 vol% C_3H_6-argon plasma reduces the calculated values of k_o and k_L (tables II and III). The high relative concentration of radicals n_R shown in position G with increasing power indicates that the polymerized species were recombining. In other words, monomer is reformed. For the $SiCl_4$-argon plasma adding either 20 vol% hydrogen or 15 vol% ammonia in positions H and G also resulted in higher relative n_R values and favorably affected k_o and k_i by increasing both the dissociation of the monomer and the formation of the polysilicon species.

The role played by hydrogen in forming free radicals from the monomers is indicated in table IV, where EPR

TABLE IV. - EPR INTENSITY RATIO FOR VARIOUS GAS MIXTURES

[Input power, 100 W; pressure, 1.0 torr; position G.]

Gas mixture ratio	EPR intensity ratio, β	Concentration, vol%
$\frac{66\ vol\%\ C_3H_4 + Ar}{16\ vol\%\ C_3H_6 + Ar}$	1.0	CH_4 - 16.0 C_3H_6 - 16.0 $SiCl_4$ - 3.5 NH_3 - 15.0 H_2 - 20.0 Ar - up to 100
$\frac{SiCl_4 + H_2 + Ar}{SiCl_4 + Ar}$	15.0	
$\frac{SiCl_4 + NH_3 + Ar}{SiCl_4 + Ar}$	10.0	
$H_2 + Ar$	(a)	
$\frac{C_3H_6 + H_2 + Ar}{C_3H_6}$	6.5	
$\frac{C_3H_6 + H_2 + Ar}{C_3H_6 + Ar}$	10.0	
$\frac{CH_4 + H_2 + Ar}{CH_4 + Ar}$	30.0	

[a]No EPR intensity measured.

intensity ratios β are given for position G at 100 W. For propylene concentrations of 16 and 66 vol%, without hydrogen added to the gas mixture, equal amounts of free radicals were formed (i.e., β = unity). In other hydrocarbon plasmas, when 20 vol% hydrogen was added to the gas stream, the amount of free radicals was enhanced by at least one order of magnitude. Similar results for β were obtained for the chlorosilanes with 20 vol% hydrogen in argon. Assuming that the amount of free radicals adsorbed on alumina represented their concentration in the plasma, the addition of 20 vol% hydrogen increased β values and promoted the free radical interaction with the monomer for the same σ_R. A higher concentration of free radicals n_R hindered the polymerization of hydrocarbons but enhanced the polymerization of chlorosilanes.

Deposition Rate on Floating and Grounded Substrates

The deposition rate (μm h^{-1}) of pyrocarbons on a graphite substrate placed in position F (position of highest deposition rate (ref. 40)) and the EPR intensity of free radicals are shown as functions of total gas pressure in a 16 vol% C_3H_6-argon plasma in figure 7. The deposition rate on the grounded substrate in the rf plasma was highest at about 7.0 torr. The maximum EPR intensity under identical conditions was obtained at 1.0 torr and decreased with increasing pressure. The deposition rate of pyrocarbon was modeled in a previous publication (ref. 51). From this model it emerged that the flux of positive ions, accelerated by the electrical field in the sheath, forms around the either grounded or negatively biased (−100 V) substrate, impinges on the substrate surface, and releases sputtered particles and secondary electrons from it. These emitted secondary electrons are accelerated in the sheath toward the plasma and form a high-energy electron beam that reacts with and ionizes the free particles in the plasma layer (ref. 51). The maximum deposition rate in figure 7 corresponds to

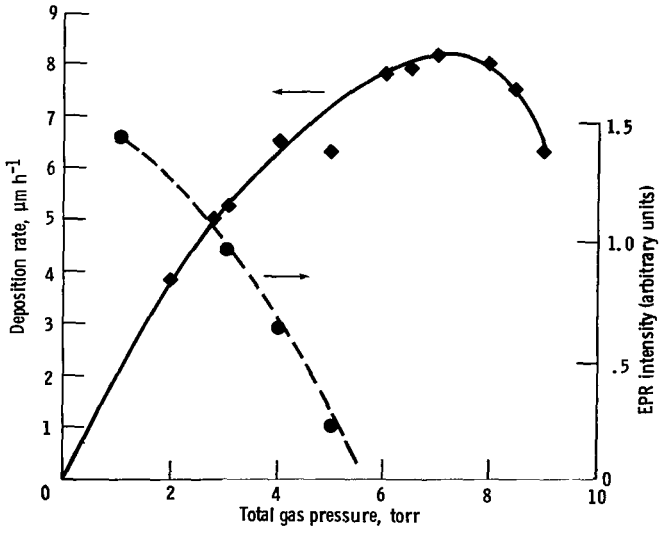

Figure 7. – Deposition rate and EPR intensity as function of total gas pressure for 16 vol% C_3H_6-argon plasma at 400 W.

TABLE V. - SILICON AND Si_3N_4 DEPOSITION RATE FROM $SiCl_4$ + Ar WITH AND WITHOUT HYDROGEN OR AMONIA ADDITION FOR IDENTICAL PLASMA CONDITIONS

[Input power, 150 W; pressure, 2 torr; position H.]

Gas mixture, vol%	Substrate connection	Deposition rate[a]	
		$\mu m\ h^{-1}$	$mg\ h^{-1}$
5 vol% $SiCl_4$ + Ar	Grounded	0.7	0.9
5 vol% $SiCl_4$ + 15 vol% H_2 + Ar	Grounded	1.4	2.3
	Floating	2.0	3.1
5 vol% $SiCl_4$ + 15 vol% NH_3 + Ar	Grounded	1.1	1.8
	Floating	1.8	3.0

[a]Measured on one side of 20- by 40-mm steel substrate to compare deposition rates for all substrates. Calculated values (for one side) of dG/dt, mg h^{-1}, or dh/dt, $\mu m\ h^{-1}$, on the grounded connection are presented.

a minimum free radical concentration; thus it might be concluded that an ion-molecule mechanism governs the deposition of pyrocarbons rather than a radical-molecule mechanism. The highest deposition rate was obtained for a 16 vol% C_3H_6-argon plasma, indicating the upper limit of propylene concentration in the gas mixture. For plasmas with higher than 16 vol% C_3H_6 concentration, which evolve higher amounts of hydrogen, the pyrocarbon deposition rate decreased continuously. Thus a high hydrogen concentration, which hinders ion-molecule reactions, decreases the pyrocarbon deposition rate. The pyrocarbon deposition rate on a floating graphite substrate was even lower (below 1.0 $\mu m\ h^{-1}$). This is in accordance with the ion-molecule mechanism shown in table V for the deposition rates of silicon and Si_3N_4. If the rate-determining step in the presence of hydrogen or ammonia was an ion-molecule mechanism, the highest deposition rate should have been obtained on a negatively biased substrate or a grounded substrate. If it was a radical-molecule mechanism, a higher deposition rate of silicon or Si_3N_4 should have been obtained on a floating substrate. As shown in table V a higher deposition rate was obtained for a floating substrate than for a grounded substrate. Thus in the presence of hydrogen or ammonia a radical-molecule mechanism governs the formation and deposition of silicon and Si_3N_4.

Conclusions

It has been shown that two mechanisms are responsible for the dissociation, polymerization, and deposition in rf plasmas of hydrocarbons and chlorosilane monomers: (1) ion-molecule interactions and (2) excited radical-molecule interactions. When argon alone is present in the two plasmas, the rate-determining step is an ion-molecule mechanism. When hydrogen or ammonia as well as argon is present in the two plasmas, the rate-determining step is a radical-molecule mechanism.

National Aeronautics and Space Administration
Lewis Research Center
Cleveland, Ohio, January 31, 1984

References

1. Bokros, J. C.: Deposition, Structure, and Properties of Pyrolytic Carbon. Chemistry and Physics of Carbon, P. L. Walker, ed., Vol. 5, Dekker, 1969, pp. 1-118.
2. Fitzer, E.; and Heym, M.: High-Temperature Mechanical Properties of Carbon and Graphite—A Review. High Temp. High Pressures, vol. 10, no. 1, 1978, pp. 29-66.
3. Fitzer, E.; et al.: Deposition of Silicon Carbide or Carbon Monofilaments. Proceedings of Fifth International Conference on Chemical Vapor Deposition. Electrochemical Society, 1975, pp. 589-599.
4. Christen, F.; Naslain, R.; and Bernard, C.: A Thermodynamic and Experimental Approach of Silicon Carbide-CVD Application to the CVD-Infiltration of Porous Carbon-Carbon Composites. Proceedings of Seventh International Conference on Chemical Vapor Deposition. Vol. 79-3, Electrochemical Society, 1979, pp. 499-514.
5. Fitzer, E.; Hegen, D.; and Strohmeier, H.: Improved Silicon Ceramics. Proceedings of Seventh International Conference on Chemical Vapor Deposition. Vol. 79-3, Electrochemical Society, 1979, pp. 525-535.
6. Sinha, A. K.; and Lugujjo, E.: Lorentz-Lorenz Correlation for Reactively Plasma Deposited Si-N Films. Appl. Phys. Lett., vol. 32, no. 4, Feb. 15, 1978, pp. 245-246.
7. Blocher, J. M., Jr.: Chemical Vapor Deposition. Deposition Technologies for Films and Coatings, R. F. Bunshah, ed., Noyes Pub., 1982, pp. 335-364.
8. Yee, K. K.: Protective Coatings for Metals by Chemical Vapour Deposition. Int. Met. Rev., vol. 23, no. 1, 1978, pp. 19-42.
9. Bryant, W. A.: The Fundamentals of Chemical Vapour Deposition. J. Mater. Sci., vol. 12, July 1977, pp. 1285-1306.

10. Bonifield, T. D.: Plasma Assisted Chemical Vapor Deposition. Deposition Technolgies for Films and Coatings, R. F. Bunshah, ed., Noyes Pub., 1982, pp. 365-384.
11. Shen, M.: Plasma Chemistry of Polymers. Dekker, 1976.
12. Rummler, D. R.: Recent Advances in Carbon-Carbon Materials Systems. Advanced Materials Technology. NASA CP-2251, 1982, pp. 293-312.
13. Miller, T. J.; and Grimes, H. H.: Research on Ultra-High-Temperature Materials, Monolithic Ceramics, Ceramic Matrix Composites and Carbon/Carbon Composites. Advanced Materials Technology. NASA CP-2251, 1982, pp. 275-292.
14. Byrd, J. A.; Janovicz, M. A.; and Thraster, S. R.: Ceramic Applications in Turbine Engines. (DDA-EDR-10672, General Motors Corp.; NASA Contract DEN3-17.) NASA CR-165494, 1981.
15. Reinberg, A. R.: Plasma Deposition of Inorganic Thin-Films. Annu. Rev. Mater. Sci., vol. 9, 1979, pp. 341-372.
16. Vossen, J. L.; and Kern, W. B., eds.: Thin Film Processes. Academic Press, 1978.
17. Yasuda, H.: Glow Discharge Polymerization. Thin Film Processes, J. L. Vossen and W. Kern, eds., Academic Press, 1978, pp. 361-398.
18. Shen, M.; and Bell, A. T.: Plasma Polymerization, ACS Symposium. Series 108, American Chemical Society, 1979.
19. Carmi, U.; et al.: The Pyrolysis of Methane in a Flowing Microwave Plasma. Pt. 1: Diagnostics, Pt. 2: Kinetics. KFA Julich Report 1499, 1978.
20. Luhleich, H.; et al.: Temperaturmessung mit einem Quotientenpyrometer Der Einfluss Unterschiedlich Heisser Oberflächenabschnitte. High Temp. High Pressures, vol. 9, no. 3, 1977, pp. 283-290.
and Polymerization of Gaseous Hydrocarbons. Plasma Chem. Plasma Processes, vol. 1, no. 4, Dec. 1981, pp. 377-395.
22. Brodsky, M. H.: Amorphous Semiconductors. Springer-Verlag, 1979.
23. Turban, G.; Catherine, Y.; and Grolleau, B.: Mass Spectrometry of a Silane Glow Discharge During Plasma Deposition of a-Si:H Films. Thin Solid Films, vol. 67, 1980, pp. 309-320.
24. Kocian, P.; Major, J. M.; and Bourguard, S.: Some Properties of a Low-Pressure Discharge in Silane. J. Phys. Colloq., 1979, pp. 169-170.
25. Knights, J. C.; et al.: Effects of Inert Gas Dilution of Silane on Plasma-Deposited a-Si:H Films. Appl. Phys. Lett., vol. 38, March 1, 1981, pp. 331-333.
26. Plattner, R. D.; et al.: Comparison of Optical and Electrical Properties of Hydrogenated a-Si Films Formed by Glow Discharge of SiH_4 or $SiCl_4/H_2$. 2nd E. C. Photovoltaic Solar Energy Conference, R. Van Overstraeten and W. Palz, eds., D. Reidel, 1979, pp. 860-866.
27. Grossman, E.; Avni, R.; and Grill, A.: Deposition of Silicon from $SiCl_4$ in an Inductive R. F. Low Pressure Plasma. Thin Solid Films, vol. 90, 1982, pp. 237-241.
28. Grimberg, A.; Grill, A.; and Avni, R.: Preparation of Polycrystalline Silicon Coatings from Trichlorosilane. Thin Solid Films, vol. 96, no. 2, Oct. 8, 1982, pp. 163-167.
29. Boonstra, A. H.; and Mutsaers, C. A. H. A.: The Effect of Particle Size on the Temperature Coefficient of Resistance of Thick Film Resistors. Thin Solid Films, vol. 67, 1980, pp. 13-20.
30. Capezzuto, P.; Bruno, G.; and Cramarossa, F.: Doped Silicon Films from $SiCl_4$-H_2 Glow Discharges. Proceedings of the 6th International Symposium on Plasma Chemistry, M. I. Boulos and R. J. Munz, eds., vol. 3, 1983, pp. 814-819.
31. Ron, Y.; et al.: Deposition of Silicon Nitride from Tetrachlorosilane and Ammonia in a Low Pressure r.f. Plasma. Thin Solid Films, vol. 107, no. 2, 1983, pp. 181-189.
32. Pliskin, W. A.: Comparison of Properties of Dielectric Films Deposited by Various Methods. J. Vac. Sci. Technol., vol. 14, no. 5, Sept./Oct. 1977, pp. 1064-1081.
33. Katz, M.; Itzhak, D.; Grill, A.; and Avni, R.: Deposition of Silicon Carbide Coatings on Titanium Alloy with a Low Pressure R. F. Plasma. Thin Solid Films, vol. 72, 1980, pp. 497-501.
34. Vasile, M. J.; and Smolinsky, G.: Mass-Spectrometric Sampling of the Ionic and Neutral Species Present in Different Regions of an RF Discharge in Methane. Int. J. Mass. Spectrom. Ion Phys., vol. 18, no. 2, Oct. 1975, pp. 179-192.
35. Vasile, M. J.; and Smolinsky, G.: The Chemistry of Radio-frequency Discharges: Acetylene and Mixtures of Acetylene with Helium, Argon and Xenon. Int. J. Mass. Spectrom. Ion Phys., vol. 24, no. 1, May 1977, pp. 11-23.
36. Vasile, M. J.; and Smolinsky, G.: The Chemistry of the Ethylene Radiofrequency Discharge. Int. J. Mass. Spectrom. Ion Phys., vol. 22, no. 1/2, Nov. 1976, pp. 171-183.
37. Calcole, H. F.: Ion-Molecule Reaction in a Gas Discharge. Presented at the International Workshop on Plasma Chemistry in Technology (Ashquelon, Israel), March 1981.
38. Turban, G.; Catherine, Y.; and Grolleau, B.: Discharge Deposition of a-Si:H Films. Ion and Radical Reactions in the Silane Glow. Plasma Chem. Plasma Processes, vol. 2, no. 1, Mar. 1982, pp. 61-80.
39. Catherine, Y.; Turban, G.; and Grolleau, B.: Neutral and Ion Chemistry in a C_2H_4-SiH_4 Discharge. Plasma Chem. Plasma Process, vol. 2, no. 1, Mar. 1982, pp. 81-93.
40. Carmi, U.; Inspektor, A.; and Avni, R.: Mechanism and Kinetics of Polymerization of Propylene in a Microwave Plasma. Plasma Chem. Plasma Process, vol. 1, no. 3, Sept. 1981, pp. 233-245.
41. Haller, I.: Importance of Chain Reactions in the Plasma Deposition of Hydrogenated Amorphous Silicon. J. Vac. Sci. Technol. A., vol. 1, no. 3, July/Sept. 1983, pp. 1376-1382.
42. Bell, A. T.: The Mechanism and Kinetics of Plasma Polymerization. Plasma Chemistry III, S. Veprek and M. Venugopalan, eds., Topics in Current Chemistry, vol. 94, Springer-Verlag, 1980, pp. 43-68.
43. Denaro, A. R.; Owens, P. A.; and Crawshaw, A.: Glow Discharge Polymerization. Eur. Polym. J., vol. 4, no. 1, 1968, pp. 93-106.
44. Tibbitt, J. M.; et al.: A Model for the Kinetics of Plasma Polymerization. Macromolecules, vol. 10, no. 3, 1977, pp. 647-653.
45. Manory, R.; et al.: Decomposition and Polymerization of Silicon Tetrachloride in a Microwave Plasma. Plasma Chem. Plasma Process, vol. 3, no. 2, 1983, pp. 235-248.
46. Field, F. H.; Franklin, J. L.; and Munson, M. S. B.: Reactions of Gaseous Ions. XII. High Pressure Mass Spectrometric Study of Methane. J. Am. Chem. Soc., vol. 85, no. 22, Nov. 20, 1963, pp. 3575-3583.
47. Bishop, W. P.; and Dorfman, L. M.: Pulse Radiolysis Studies. XVI. Kinetics of the Reaction of Gaseous Hydrogen Atoms with Molecular Oxygen by Fast Lyman-α Absorption Spectrophotometry. J. Chem. Phys., vol. 52, no. 6, Mar. 15, 1970, pp. 3210-3216.
48. Magnotta, F.; Nesbitt, D. J.; and Leone, S. R.: Excimer Laser Photolysis Studies of Translational-to-Vibrational Energy Transfer. Chem. Phys. Lett., vol. 83, no. 1, Oct. 1, 1981, pp. 21-25.
49. McDaniel, E. W. Collision Phenomena in Ionized Gases. Wiley, 1964.
50. Chapman, B. N.: Glow Discharge Processes: Sputtering and Plasma Etching. Wiley, 1980.
51. Khait, Y. L.; Inspektor, A.; and Avni, R.: The Dependence of Coating in Inductive R.F. Plasmas on Gas Flow Velocity, Pressure and R. F. Power. Thin Solid Films, vol. 72, 1980, pp. 249-260.

1. Report No.	2. Government Accession No.	3. Recipient's Catalog No.
NASA TP-2301		

4. Title and Subtitle	5. Report Date
Homogeneous Reactions of Hydrocarbons, Silane, and Chlorosilanes in Radiofrequency Plasmas at Low Pressures	April 1984
	6. Performing Organization Code: 506-53-1B
7. Author(s): Reuven Avni, Uzi Carmi, Aron Inspektor, and Ionel Rosenthal	8. Performing Organization Report No.: E-1919
	10. Work Unit No.
9. Performing Organization Name and Address: National Aeronautics and Space Administration, Lewis Research Center, Cleveland, Ohio 44135	11. Contract or Grant No.
	13. Type of Report and Period Covered: Technical Paper
12. Sponsoring Agency Name and Address: National Aeronautics and Space Administration, Washington, D.C. 20546	14. Sponsoring Agency Code

15. Supplementary Notes

Presented in part at Sixth International Symposium on Plasma Chemistry, sponsored by the International Union of Pure and Applied Chemistry, Montreal, Canada, July 24-28, 1983. Reuven Avni, Nuclear Research Center Negev, Beer Sheva, Israel, and National Research Council - NASA Research Associate; Uzi Carmi, Aron Inspektor, and Ionel Rosenthal, Nuclear Research Center Negev, Beer Sheva, Israel.

16. Abstract

The ion-molecule and radical-molecule mechanisms are responsible for the dissociation of hydrocarbon, silane, and chlorosilane monomers and the formation of polymerized species, respectively, in an rf plasma discharge. In a plasma containing a mixture of monomer and argon the rate-determining step for both dissociation and polymerization is governed by an ion-molecule type of interaction. Adding hydrogen or ammonia to the monomer-argon mixture transforms the rate-determining step from an ion-molecule interaction to a radical-molecule interaction for both monomer dissociation and polymerization.

17. Key Words (Suggested by Author(s))		18. Distribution Statement
Plasma processing	Chlorosilanes	Unclassified - unlimited
Mechanism	Dissociation	STAR Category 23
Hydrocarbons	Polymerization	
Silanes		

19. Security Classif. (of this report)	20. Security Classif. (of this page)	21. No. of pages	22. Price*
Unclassified	Unclassified	12	A02

*For sale by the National Technical Information Service, Springfield, Virginia 22161

NASA-Langley, 1984

National Aeronautics and
Space Administration

Washington, D.C.
20546

Official Business
Penalty for Private Use, $300

THIRD-CLASS BULK RATE

Postage and Fees Paid
National Aeronautics and
Space Administration
NASA-451

1 1U,C, 840322 S00903DS
DEPT OF THE AIR FORCE
AF WEAPONS LABORATORY
ATTN: TECHNICAL LIBRARY (SUL)
KIRTLAND AFB NM 87116

NASA

POSTMASTER: If Undeliverable (Section 158 Postal Manual) Do Not Return